Characterization of Bacterial Community Structure on a Weathered Pegmatitic Granite

Deirdre B. Gleeson[1], Nabla M. Kennedy[1], Nicholas Clipson[1], Karrie Melville[2], Geoffrey M. Gadd[2] and Frank P. McDermott[3]

(1) Microbial Ecology Group, School of Biology and Environmental Science, University College Dublin, Belfield, Dublin 4, Ireland
(2) Division of Environmental and Applied Biology, Biological Sciences Institute, School of Life Sciences, University of Dundee, Dundee DD1 4HN, Scotland, UK
(3) School of Geological Sciences, University College Dublin, Belfield, Dublin 4, Ireland

Abstract

This study exploited the contrasting major element chemistry of a pegmatitic granite to investigate mineralogical influences on bacterial community structure. Intact crystals of variably weathered muscovite, plagioclase, K-feldspar, and quartz were extracted, together with whole-rock granite. Environmental scanning electron microscopy revealed a diversity of bacterial structures, with rods and cocci clearly visible on surfaces of all mineral types. Bacterial automated ribosomal intergenic spacer analysis was used to generate a ribotype profile for each mineral. A randomization test revealed that community fingerprints differed between different mineral types, whereas canonical correspondence analysis (CCA) showed that mineral chemistry affected individual bacterial ribotypes. CCA also revealed that Al, Si, and Ca had a significant impact on bacterial community structure within the system, which contrasts with the finding within fungal communities that although Al and Si also had a significant impact, K rather than Ca was important. The bacterial populations associated with different minerals were different. Members of each of these populations were found almost exclusively on a single mineral type, as was previously reported for fungal populations. These results show that bacterial community structure was driven by the chemical composition of minerals, indicating selective pressure by individual chemical elements on bacterial populations *in situ*.

Introduction

Mineral weathering is a key global process in the formation of soils and sediments, in determining the chemical composition of aquatic environments, and in the long-term regulation of Earth's climate. It is increasingly recognized that there is a strong biological component in many weathering processes [2, 3, 5, 12, 22, 26]. Cyanobacteria, chemoorganotrophic and chemolithotrophic bacteria, algae, and fungi are all important components of rock microbial communities, and their combined activity appreciably alters rates of rock surface disintegration. Microcosm-based studies using scanning (SEM) and transmission electron microscopy (TEM) and light microscopy have revealed microbial colonies on silicate glass and aluminosilicate surfaces [4, 21, 23, 24, 26, 28], but little is known about the extent to which mineralogy exerts selective pressure on indigenous microbial communities.

Silicate minerals are the principal components of igneous rocks, including the pegmatitic Caledonian granites that are the subject of this study. There has been much interest in the weathering of silicate minerals [6, 21], with microbial–mineral interactions perturbing surface reaction dynamics through the production of protons, hydroxyl ions, or metal-chelating metabolic products [21]. Microbial involvement in surface processes has been considered at a microenvironmental level,

with localized chemical environments being very different from those of bulk solutions, often resulting in localized etching [13, 24]. Key questions concerning microbial activity in surface weathering processes of silicates are the degree to which microbial populations target specific silicate minerals and the extent to which microbes derive nutrition from silicate weathering.

Until recently, estimates of bacterial community diversity have been problematic due to the inherent biases of culture-based microbiology, with media selecting for copiotrophic microbial populations [1]; it is thought that less than 5% of microbial species can be cultured [25]. The advent of molecular methods based upon cloning [8] or genetic fingerprinting [7, 20], has allowed much more detailed analysis of bacterial communities, and in particular bacterial community structure, in natural environments. Methods such as automated ribosomal intergenic spacer analysis (ARISA), in which the 16S–23S spacer region is amplified, discriminate to species or even strain level, giving rise to its increased use in the analysis of bacterial diversity.

In this study, we exploited the contrasting major element chemistry of adjacent physically separable crystals of framework and sheet silicates in a pegmatitic granite to investigate controls on bacterial diversity on mineral surfaces. Pegmatite was selected because its constituents are major rock-forming minerals, and their large grain sizes facilitate physical separation for analysis. A DNA-based community fingerprinting approach [ribosomal intergenic spacer analysis (RISA)] combined with sequencing was used to identify some of the constituent bacterial populations. ARISA was used to generate a bacterial ribotype profile for each mineral type, consisting of the individual ARISA amplicons present and their relative abundances. These data were then combined with elemental analysis of minerals together with multivariate statistics to identify those chemical properties of the constituent pegmatite silicates that significantly influence bacterial community structure.

In a companion paper to this study we showed a strong substrate control on fungal community structure, with many fungal populations being limited to a single mineral type [14]. As both bacteria and fungi are important components of rock microbial communities, it is important to elucidate the chemical factors influencing both communities. As can be seen from this study, Al, Si, and Ca had a significant impact on bacterial community structure, and although Al and Si also had a significant impact on fungal community structure, K rather than Ca was important. In this study we use DNA-based approaches, which have not been applied previously to assess bacterial diversity on mineral surfaces. We report a strong substrate control on bacterial community structure, with many bacterial populations being limited to a single mineral type.

Methods

Study Area and Sampling Procedure. Large intact crystals (four replicate samples of each) of variably weathered muscovite, plagioclase, K-feldspar, and quartz were individually extracted, together with whole-rock granite, from the surface of a single decimeter-scale pegmatite vein. The pegmatite occurred as a single weathered outcrop, approximately 10 m in length, in an area of Caledonian granite (ca. 400 million years old) from the Wicklow Mountains, Ireland (grid ref: O 127113). All samples were removed immediately to the laboratory and were stored at 4°C (for chemical analysis) or at −20°C (for molecular analysis).

Environmental Scanning Electron Microscopy. Samples for environmental scanning electron microscopy (ESEM) were sputter-coated with 40 nm Au/Pd and visualized using a Philips XL30 environmental scanning electron microscope. Images were examined for evidence of microbial attachment, the types of microorganisms present, as well as the pattern and extent of microbial colonization.

Major Element Chemistry. Small portions of the weathered surfaces of each sample were powdered using a tungsten carbide mill and their major element compositions were determined on fused glass beads by wavelength dispersive X-ray fluorescence (XRF) using standard techniques [19].

Total Rock DNA Extraction and Purification. Total rock DNA extraction was based on the method of Gleeson et al. [14]. DNA was consistently suitable for polymerase chain reaction (PCR) amplification without further treatment.

Bacterial RISA. RISA PCR was performed by using a modification of the method of Ranjard et al. [20]. After extraction and purification of total DNA from the weathered rock or mineral samples, the intergenic spacer (ITS) region between the 16S and 23S rRNA genes was amplified by using primer set S-D-Bact-1522-b-S-20 (eubacterial rRNA small subunit, 5′-TGCGGCTGGATC CCCTCCTT-3′) and L-D-Bact-132-a-A-18 (eubacterial rRNA large subunit, 5′-CCGGGTTTCCCCATTCGG-3′) [18]. PCR reaction mixtures were performed in 50-μL volumes containing 1× Mg-free PCR buffer (Sigma-Aldrich), 2.5 mM $MgCl_2$ (Sigma-Aldrich), 15 pmol of each primer (MWG Biotech), 200 μmol of each dNTP (Sigma), and ~10 ng extracted total rock DNA and 2.5 U *Taq* DNA polymerase (Sigma-Aldrich). A hot start of 94°C for 3 min was performed prior to addition of *Taq* DNA polymerase. Reaction mixtures were then held at 94°C for 2 min, followed by 30 cycles of amplification at

94°C for 1 min, 55°C for 30 s, 72°C for 1 min, and a final extension of 72°C for 5 min.

RISA Amplicon Sequencing. RISA amplicons were electrophoresed (CBS Scientific, UK) on a nondenaturing polyacrylamide gel at 85 V for 12 h at 25°C with $1\times$ TAE buffer. Gels were stained with SYBR Green™ (Sigma-Aldrich), viewed under UV and individual bands excised. DNA was extracted from gels by bead-beating in 100 µL of TE buffer (1.0 M, pH 8.0) at 5.5 ms^{-1} for 30 s, followed by diffusion into sterile water at 4°C overnight. Each band was then reamplified by using the original primer set. The reamplified PCR products were verified by agarose gel electrophoresis and further purified by using a High Pure™ PCR product cleanup kit and then sequenced by using the original forward primer. DNA sequencing was carried out by MWG-Biotech, and sequence analysis and homology searches (BLAST) were conducted at the network server of the National Center for Biotechnology Information.

Bacterial Community Fingerprinting by ARISA. ARISA involved the use of a fluorescently labeled primer for PCR. The forward primer, S-D-Bact-1522-b-S-20, was labeled with Beckman Coulter fluorescent dye D4. PCR products were first visualized on a 1.2% agarose gel, then purified by using a High Pure PCR product purification kit and eluted in 50 µL of sterile water (heated to 50°C). The purified PCR products were quantified on a 1.2% agarose gel before mixing aliquots (0.5–1 µL) with 38.4 µL of deionized formamide, 0.2 µL of Beckman Coulter size standard 600 (dye D1), and 0.4 µL of custom-made marker containing DNA fragments of 600, 620, 640, 660, 680, 700, 720, 740, 760, 780, 800, 820, 840, 860, 880, 900, 920, 940, 960, 980, 1000, 1050, 1100, 1150, and 1200 bp, all labeled with Beckman Coulter Dye D1 (BioVentures, Murfreesboro, TN, USA). Intergenic spacer lengths were determined by electrophoresis using a Beckman Coulter (CEQ8000) automated sequencer, version 6.0.2 (High Wycombe, Bucks, UK) (resolution ± 1 bp up to 400 bp ribotype length, ± 2 bp thereafter).

Run conditions were 60°C separation temperature, 4 kV voltage, and 120 min separation time to allow for separation of the larger fragments.

Analysis of ITS-amplicon profiles was performed by using a Beckman Coulter fragment-analysis package (v.4.0). Only amplicons with a fluorescence greater than 1% of the total fluorescence were included in the analyses. A quartic polynomial model rather than the recommended cubic model was used for size calibration, as this resulted in improved correlation between expected and actual size of standard fragments, particularly for amplicons in the range 1000–1200 bp. ARISA amplicons that differed by less than 0.5 bp in different profiles were considered identical. Amplicon lengths that were present in each of two replicates were used to produce a representative ARISA profile of each bacterial community. In order to make comparisons of microbial communities more reliable, a modification of an analytical procedure proposed by Dunbar *et al.* [11] was used. This approach reduces the variation due to mainly small irreproducible peaks and extracts a reproducible subset of data from replicate ARISA profiles. The peak heights of individual ARISA amplicons were relativized as a percentage of their abundance within a sample in order to account for DNA quality differences between replicate profiles.

Phylogenetic Analysis. The GenBank database (National Center for Biotechnology Information) was searched for sequence similarity of the 16S–23S rRNA ITS with sequences obtained in this study. The most similar sequences were used for multiple sequence alignments with Clustal W (http://www.ebi.ac.uk/clustalw/). ITS sequences obtained in this study were included in the analysis. MEGA 2.0 (Molecular Evolutionary Genetics Analysis [17]) was used to generate a neighbor-joining tree based on distance matrix analysis of the aligned 400-bp sequences, with *Escherichia coli* as the outgroup. The stability of the groupings was checked by bootstrap analysis of 1000 replications. The ITS sequences obtained in this study have been deposited in the GenBank database under the accession numbers AY534289–AY534294 and AY533029.

Statistical Analyses. Sample ribotype profiles were compared using a variation of the cityblock randomization test procedure [16]. Genstat (version 6)

Table 1. XRF of the major element composition (weight percent) of each mineral (mean of four replicates)

Sample	Al_2O_3	K_2O	Na_2O	CaO	Fe_2O_3	SiO_2	MgO	P_2O_5
Granite	15.81	4.42	3.22	0.62	1.06	72.68	0.27	0.13
Muscovite	35.55	9.73	0.73	0.04	2.77	49.33	0.57	0.19
K-Feldspar	18.76	13.86	1.71	0.15	0.11	64.31	0.05	0.01
Plagioclase	19.50	0.50	10.64	0.05	0.10	68.94	0.04	0.01
Quartz	0.07	0.01	0.01	0.02	0.03	99.80	0.03	0.01

Detection limits are typically 0.01 wt%.

was used to calculate the overall abundance of each individual ribotype for all samples. Ribotypes were then ranked according to overall abundance and these rankings used to select ribotypes for inclusion in multivariate analysis. Canonical correspondence analysis (CCA) using Canoco for Windows (version 4.02) was used to analyze ARISA data, based on initial analysis by detrended correspondence analysis revealing that data exhibited a unimodal rather than linear distribution [15]. The resulting ordination biplot approximated the
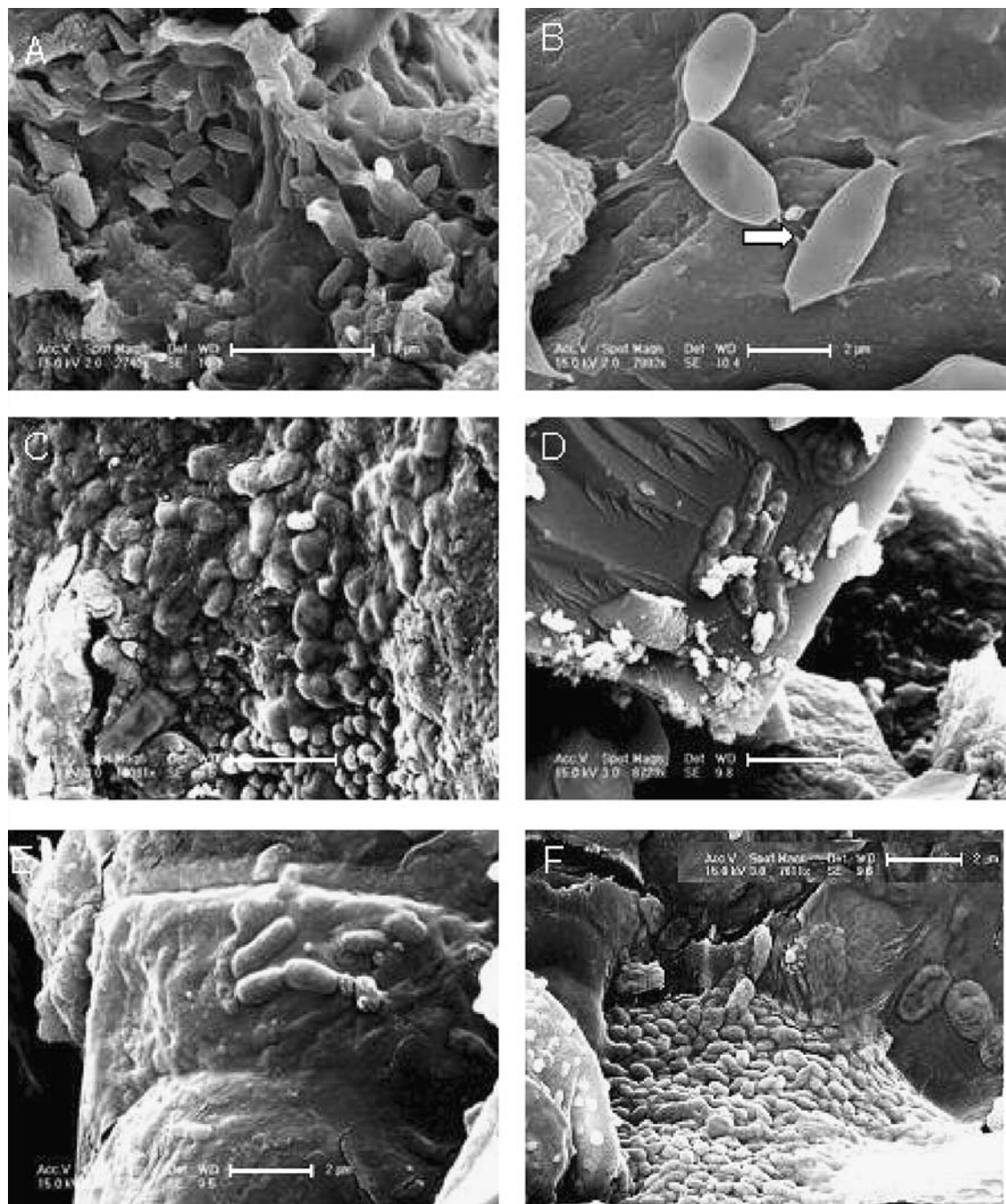
Figure 1. ESEMs of mineral surfaces. (A) ESEM of muscovite surface showing rod-shaped bacterial cells, approximately 1.5 μm in diameter (bar marker = 10 μm). (B) ESEM of muscovite showing single bacterial cells with cellular adhesion appendages (*arrowed*) visible (bar marker = 2 μm). (C) ESEM of K-feldspar surface with bacterial mat covering the mineral surface (bar marker = 2 μm). (D) ESEM of K-feldspar surface with bacterial cells (approx. 1 μm in length) present on smooth mineral surface (bar marker = 2 μm). (E) ESEM of plagioclase with visible rod-shaped bacterial cells (bar marker = 2 μm). (F) ESEM of quartz surface with bacterial mat covering surface (bar marker = 2 μm).

Table 2. Results of CCA for the 28 most abundant ribotypes

Axis	1	2
Eigenvalue	0.973	0.833
Cumulative percentage variance		
Of ribotype	14.1	26.2
Of ribotype–chemical relation	23.7	44.0
Ribotype–chemical correlations	0.998	0.994
Monte Carlo significance test		For all axes:
F ratio	1.809	2.024
P value	0.005	0.005
Correlations ($100 \times r$)		
Al	**−74.94**	+38.72
Si	**+72.78**	+45.51
K	−30.43	**69.69**

Values are for axes 1 and 2 plotted in the CCA diagram in Fig. 2. The highest canonical correlations are highlighted in bold.

weighted average of each species (in this case, relative abundances of ribotypes) with respect to each of the chemical factors, which were represented as arrows. The length of these arrows indicated the relative importance of that chemical factor in explaining variation in bacterial profiles, whereas the angle between arrows indicated the degree to which they were correlated. A Monte Carlo permutation test based on 199 random permutations was used to test the null hypothesis that bacterial profiles were unrelated to environmental variables. The 28 most abundant ribotypes were also analyzed by one-way analysis of variance (ANOVA) using SPSS (version 10) to determine which chemical factors had a significant effect.

Results

Chemical Analysis. Major element analyses of whole weathered granite and individual large crystals of its constituent minerals (muscovite, K-feldspar, plagioclase, and quartz) are shown in Table 1. Elemental compositions of the mica and feldspar minerals were typical of those associated with granitic lithologies [10].

Environmental Scanning Electron Microscopy. ESEM analysis of the rock and mineral samples revealed a diversity of microbiological structures, including bacteria and fungi. Representative micrographs of bacterial communities are shown in Fig. 1. Rod-shaped bacteria were present on the surfaces of all minerals examined, and occurred either singly or as a bacterial mat.

Bacterial Community Profiles. ARISA was used to generate bacterial ribotype profiles for each mineral type, consisting of the individual ARISA amplicons present and their relative abundances. Each ARISA amplicon indicated one sequence polymorphism, or ribotype. Average sample ribotype numbers ranged from 22 on granite, 18 on muscovite, 16 on K-feldspar and plagioclase, to 10
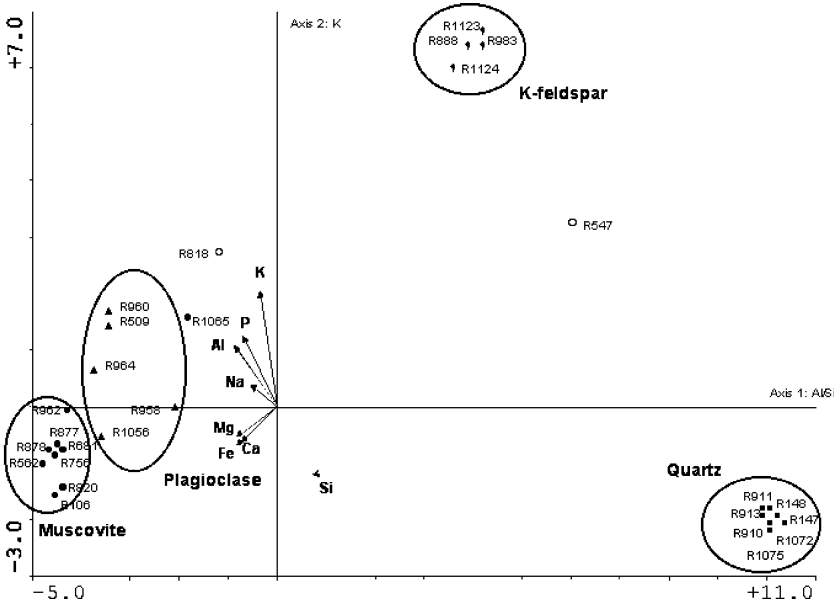

Figure 2. CCA ordination bacterial ARISA ribotypes in relation to measured chemical variables. The 28 most abundant bacterial ribotypes from ARISA are shown as *dots*, with chemical variables represented as *arrows*. The first canonical axis (eigenvalue 0.973, P<0.05) explains 14.1% of the total variation in the data, and is primarily correlated with Al and Si. The second axis (eigenvalue 0.833, P<0.05) explains a further 12.1% of total variation (total 26.2% for both axes), and is primarily correlated with K. Ribotype–chemical correlations for both axes were above 0.99. Correlations between specific ribotypes and chemical compositions of minerals can be visualized by noting the position of ribotypes in relation to the direction of arrows for chemical variables. Ribotypes are labeled according to size (base pairs), and have been coded as follows: • (*filled circles*), muscovite; ▲ (*filled triangles*), plagioclase; ♦ (*filled diamonds*) K-feldspar; ■ (*filled squares*) quartz; ○ (*open circles*) granite.

on quartz. It should be noted that amplicons were only included in data sets to estimate ribotype numbers if they exceeded 1% of total abundance within the sample and appeared in more than two (of four) replicates [11]. ARISA profiles were initially analyzed using a randomization test [16], which indicated that bacterial community structure differed significantly between all individual minerals ($P<0.05$; data not shown). As the randomization test required the use of multiple comparisons, a multivariate approach was then used to explore the data further. CCA was used to reveal broad-scale chemical and mineralogical influences on bacterial community structure.

CCA of all ARISA profiles, combined with major element (Si, Al, K, P, Na, Mg, Ca, Fe) compositions of mineral separates, was carried out. Initially, all ribotypes were included in CCA; however, to explore the influences of the most dominant ribotypes, the analysis was restricted to the 28 most abundant ribotypes accounting for 50% of the total bacterial abundance. Comparison of results from CCA revealed only minor changes in axes scores (data not shown) after limiting the data set to the 28 most abundant ribotypes, indicating that the 28 most abundant ribotypes accounted for the majority of the variance in the data.

Table 2 details CCA results, with high eigenvalues for axes 1 and 2 (0.973 and 0.829, respectively), indicating that the analysis accounted for a significant (Monte Carlo test, $P<0.005$) percentage of the overall variance in the ribotype data. This was supported by calculations of the cumulative percentage variance, which indicated that axes 1 and 2 together explained 26.2% of the variance within bacterial profiles. The cumulative ribotype–chemical relation for axes 1 and 2 was 44.9%, indicating that these axes accounted for almost half of the variance in bacterial community profiles attributable to chemical factors.

Figure 2 plots the 28 most abundant ribotypes in relation to all measured chemical factors. Canonical intraset correlations for the chemical factors for each axis indicated that axis 1 was most strongly correlated with Si and Al, and axis 2 with K. Correlations between specific ribotypes and chemical compositions of minerals can be visualized by noting the position of ribotypes in relation to the direction of arrows for chemical variables. Mineral type was also used to delineate groupings of ribotypes (coded on Fig. 2). Essentially four strong groupings of the 28 most abundant ribotypes were evident, with one cluster associated with quartz and correlated to Si, another associated with K-feldspar and principally correlated to K, another associated with

Table 3. ANOVA of the ribotypes accounting for 50% of the overall abundance (28 ribotypes in total) and percentage abundance of the 28 most abundant ribotypes from all mineral surfaces (accounting for 50% of overall abundance)

Ribotype No.	% Abundance	Cumulative % abundance	Significant factor ($P<0.05$)	Mineral having ribotype present
1056	3.81	3.81	NS	Plagioclase
878	3.48	7.29	Fe	Muscovite
911	3.19	10.48	NS	Quartz
964	2.94	13.42	Al	Plagioclase
1072	2.42	15.84	NS	Quartz
562	2.22	18.06	NS	Granite
818	2.19	20.25	NS	Muscovite, K-feldspar, Plagioclase
960	2.05	22.29	Al, P	Plagioclase
888	2.04	24.33	K, Na	K-feldspar
958	2.01	26.34	P	Plagioclase
547	1.88	28.23	NS	K-feldspar, Quartz
106	1.85	30.08	Ca, Fe	Muscovite
820	1.80	31.88	Ca	Muscovite
877	1.76	33.64	Ca, Fe	Muscovite
756	1.71	35.35	Fe	Muscovite
910	1.55	36.90	NS	Quartz
681	1.43	38.33	Ca	Granite
962	1.42	39.75	NS	Muscovite
913	1.38	41.13	Si	Quartz
1055	1.27	42.40	NS	Plagioclase
983	1.24	43.64	K, Fe, Na	K-feldspar
148	1.23	44.87	Si	Quartz
147	1.22	46.08	NS	Quartz
1124	1.19	47.27	Na, Ca	K-feldspar
1065	1.18	48.45	NS	Muscovite
1123	1.18	49.63	K, Na	K-feldspar
1075	1.16	50.79	NS	Quartz
509	1.16	51.96	NS	Plagioclase

Also included is a list of chemical factors significantly affecting (+ or −) individual ribotype abundance, together with the mineral type on which an individual ribotype was found. NS, not significant.
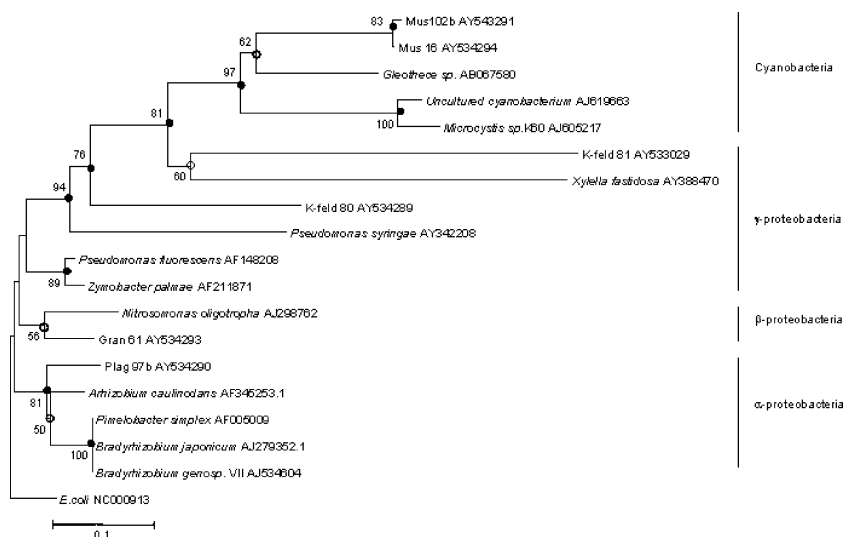
Figure 3. Phylogenetic tree. Molecular evolutionary genetics analysis (MEGA) 2.0 [17] was used to generate a neighbor-joining tree based on distance matrix analysis of the aligned 400-bp sequences, with *E. coli* as the outgroup. The stability of the groupings was checked by bootstrap analysis of 1000 replications. Accession numbers of all sequences are included. The scale bar represents 0.1 substitutions per base position. Bootstrap values are presented at nodes (*filled circle* where they exceed 70; *open circle* where they exceed 50). *musc*, muscovite; *plag*, plagioclase; *gran*, granite; *quar*, quartz; *K-feld*, K-feldspar, in reference to the mineral type from which each sequence was found.

plagioclase and principally correlated to Al, and another associated with muscovite and principally correlated to Fe. Specific ribotypes occurred exclusively on a single mineral type, with just two exceptions (R547 and R818). Correlations between specific ribotypes and chemical composition were explored further by ANOVA of individual ribotype abundances, with results detailed in Table 3. Mineral chemistry affected abundances of individual bacterial ribotypes, with evidence for both positive and negative interactions, indicating localized control of rock surface bacterial populations. In some cases, no significant correlating factor was determined for specific ribotypes, this may be due to a general abundance of these particular ribotypes, where mineral chemistry has no specific positive or negative influence.

Phylogenetic Analysis.   To obtain amplicons for sequencing and phylogenetic analysis, ITS-PCR was performed using nonfluorescently labeled primers. Amplicon mixtures were separated by polyacrylamide gel electrophoresis, and resulting bands were excised, reamplified and sequenced. Seven bands were successfully sequenced, aligned using Clustal W, and a phylogenetic tree was created using MEGA 2.0 (Fig. 3). Sequences were distributed in the proteobacteria (α, β, and γ) and the cyanobacteria. Nevertheless, it should be noted that, based on the numbers of ribotypes identified by ARISA, the successfully sequenced bands represented only a small proportion of total bacterial populations.

Discussion

Microbial involvement in chemical weathering is well established, although relatively little is known about the diversity of indigenous bacterial communities on oligotrophic silicate surfaces. In contrast with previous studies that have relied largely on microscopy, a DNA-based community profiling approach was used. Although the microcosm-based studies using SEM, TEM and light microscopy observe microbial colonies on aluminosilicate surfaces [2, 22–24, 26, 28], observations of natural microbial communities on constituent minerals of pegmatite (granitic) rocks are rare. In this study, both bacterial and fungal cells could be visualized by SEM, with bacteria sometimes being associated with etch and pit marks on mineral surfaces and with fungal hyphae. Most bacteria appeared to be rod shaped and occurred either singly or as a bacterial mat. Figure 1B shows a close-up of single rod-shaped bacterial cells, where cellular adhesion appendages are clearly visible. Fungal hyphal networks and microcolonial forms were extensive and were present on all surfaces examined, evidence of which can be seen in Gleeson *et al.* [14].

Profiling bacterial populations by molecular methods overcomes the problems of bias that occur from culturing, through either media selectivity or bacterial unculturability. Many estimates have been made for levels of microbial culturability from natural environments, with figures typically in the range of 1–5% [25]. Ribotype numbers in this study ranged from 10 to 22,

dependent on mineral type, with quartz having a less complex bacterial community structure than the other minerals. Quartz is essentially pure silica, which may restrict bacterial nutrition more than the other minerals (in terms of inorganic mineral nutrients such as K, etc.) leading to a simpler community structure, although surficial contaminants on quartz crystals may contribute to bacterial nutrition.

Community fingerprinting approaches such as ARISA produce highly complex data sets that can be difficult to interpret without recourse to multivariate statistics. Such approaches allow identification of correlations between individual ribotypes within complex community profiles and environmental variables such as mineral elemental composition. Although molecular approaches give a more extensive view of bacterial populations compared to culture-based approaches, some caution regarding the interpretation of molecular-based fingerprint data is necessary because of species differences in rRNA gene copy numbers [9] and biases in DNA extraction and PCR amplification [27].

On the basis of a randomization test, bacterial community structure was found to differ significantly ($P < 0.05$) between communities on the different mineral types sampled. XRF analysis demonstrated substantial differences between elemental contents of mineral types, as widely observed for rock-forming silicates [10]. CCA was performed using the 28 most abundant ribotypes (representing 50% of total abundance) and revealed that mineral chemistry was found to affect individual bacterial ribotypes (Fig. 2). Strong relationships were found between certain ribotypes and particular chemical elements. Correlations between specific ribotypes and chemical compositions of minerals can be visualized by noting the position of ribotypes in relation to the direction of arrows for chemical variables on the ordination diagram. Importantly, individual ribotypes were largely restricted to single mineral types, with the exception of two ribotypes (R547 and R818), and clustered strongly within the ordination diagram on the basis of mineral type. To explore interactions between individual ribotypes and mineral composition, ANOVA was performed to identify chemical factors significantly correlated with individual ribotypes (Table 3). For example, ribotype number 960, found only on plagioclase, is significantly positively correlated with aluminum and phosphorus. This compares well with similar work on fungal communities, in which specific ribotypes were found on single mineral types and in which ribotype distribution correlated with specific minerals [14]. Although culture-based approaches and microscopy have suggested that there are correlations between microbial diversity and mineral composition, these data for the first time show statistically significant mineralogical controls on *in situ* rock inhabiting bacterial populations. It suggests that specific bacterial populations are confined to particular mineral types to which they remain restricted. This finding has also been reported for fungal populations within the same system [14].

On rock surfaces, bacterial populations probably exist within biofilm communities [3] whose surface accumulation of microbial polymers has been documented [2, 26]. In this study, it was notable that sampled mineral crystals were in close proximity and were on a near-vertical slope with water percolating over surfaces. Nevertheless, distinct communities were evident in adjacent coarse crystals in the pegmatitic granite. Although water-borne transport of bacterial cells between minerals is likely, at least for some bacterial populations, some of the minerals do not appear to support growth. It might be hypothesized that if bacterial transport is widespread over these surfaces, bacterial communities on mineral surfaces may be largely determined by their inability to colonize particular surfaces on the basis of their chemical composition. Nevertheless, some caution must be expressed in interpretation, as the chemical analyses were restricted to the major elements, and other less abundant trace inorganic or organic constituents may also be influential.

In summary, analysis of bacterial community structure demonstrated that distinct bacterial populations existed on surfaces of different mineral types on a pegmatitic granite outcrop surface, with many ribotypes restricted to a single mineral type. There was strong evidence that bacterial community structure was driven by the chemical composition of mineral substrates, leading to the postulation that individual chemical elements exert selective pressure on bacterial populations *in situ*. These findings have important implications for the understanding of chemical weathering processes because a component of differential weathering of individual minerals may be attributed to their different indigenous bacterial communities.

References

1. Amman, L (1995) Phylogenetic identification and *in situ* detection of individual cells without cultivation. Microbiol Rev 59: 143–169

2. Barker, WW, Banfield, JF (1996) Biologically versus inorganically mediated weathering reactions: relationships between minerals and extracellular microbial polymers in lithobiontic communities. Chem Geol 132: 55–69

3. Barker, WW, Welch, SA, Banfield, JF (1997) Geomicrobiology of silicate mineral weathering. Rev Miner 35: 391–428

4. Barker, WW, Welch, SA, Chu, S, Banfield, JF (1998) Experimental observations of the effects of bacteria on aluminosilicate weathering. Am Mineral 83: 1551–1563

5. Bennett, PC, Hiebert, FK, Choi, WJ (1996) Microbial colonisation and weathering of silicates in a petroleum-contaminated groundwater. Chem Geol 132: 45–53

6. Bennett, PC, Rogers, JR, Choi, WJ (2001) Silicates, silicate weathering and, microbial ecology. Geomicrobiol J 18: 3–19

7. Brodie, E, Edwards, S, Clipson, N (2002) Bacterial community dynamics across a floristic gradient in a temperate upland grassland ecosystem. Microbial Ecol 44: 260–270

8. Chelius, MK, Moore, JC (2004) Molecular phylogenetic analysis of Archaea and Bacteria in Wind Cave, South Dakota. Geomicrobiol J 21: 123–134

9. Crosby, LD, Criddle, CS (2003) Understanding bias in microbial community analysis due to *rrn* operon copy number heterogeneity. Biotechniques 34: 790–802

10. Deer, WA, Howie, RA, Zussman, J (1993) An Introduction to the Rock-Forming Minerals. Longman Scientific and Technical Press, New York, p 696

11. Dunbar, J, Ticknor, LO, Kuske, CR (2001) Phylogenetic specificity and reproducibility and new method for analysis of terminal restriction fragment profiles of 16S rRNA genes from bacterial communities. Appl Environ Microbiol 67: 190–197

12. Ehrlich, HL (1998) Geomicrobiology: its significance for geology. Earth Sci Rev 45: 45–60

13. Fisk, MR, Giovannoni, SJ, Thorseth, IH (1998) Alteration of oceanic volcanic glass: textural evidence of microbial activity. Science 281: 978–980

14. Gleeson, DB, Kennedy, NM, Clipson, N, Melville, K, Gadd, GM, McDermott, PF (2005) Characterization of fungal community structure on a weathered pegmatitic granite. Microb Ecol 50: 360–368

15. Jongman, RHG, Ter Braak, CJF, van Tongeren, OFR (2004) Data Analysis in Community and Landscape Ecology. Cambridge University Press, Cambridge, UK, p 137

16. Kennedy, N, Brodie, E, Connolly, J, Clipson, N (2004) Impact of lime, nitrogen, and plant species on bacterial community structure in grassland microcosms. Environ Microbiol 6: 1070–1080

17. Kumar, S, Tamura, K, Nei, M (1993) MEGA: Molecular Evolutionary Genetics Analysis. The Pennsylvania State University, University Park

18. Normand, P, Ponsonnet, C, Nesme, X, Neyra, M, Simonet, P (1996) ITS analysis of prokaryotes. In: Akkermans, DL, van Elsas, JD, De Bruijn, EL (Eds.) Molecular Microbial Ecology Manual. Kluwer Academic Publishers, Amsterdam, pp 1–12

19. Ramsey, MH, Potts, PJ, Webb, PC, Watkins, P, Watson, JS, Coles, BJ (1995) An objective assessment of analytical method precision: comparison of ICP–AES and XRF for the analysis of silicate rocks. Chem Geol 124: 1–19

20. Ranjard, L, Poly, F, Lata, JC, Thioulouse, J, Nazaret, S (2001) Characterisation of bacterial and fungal soil communities by automated ribosomal intergenic spacer analysis fingerprints: biological and methodological variability. Appl Environ Microbiol 67: 4479–4487

21. Rogers, JR, Bennett, PC (2004) Mineral stimulation of subsurface microorganisms: release of limiting nutrients from silicates. Chem Geol 203: 91–108

22. Rogers, JR, Bennett, PC, Choi, WJ (1998) Feldspars as a source of nutrients for microorganisms. Am Mineral 83: 1532–1540

23. Santelli, CM, Welch, SA, Westrich, HR, Banfield, JF (2001) The effect of Fe-oxidizing bacteria on Fe-silicate mineral dissolution. Chem Geol 180: 99–115

24. Thorseth, IH, Furnes, H, Tumyr, O (1995) Textural and chemical effects of bacterial activity on basaltic glass: an experimental approach. Chem Geol 119: 139–160

25. Torsvik, V, Lise, O (2002) Microbial diversity and function in soil: from genes to ecosystems. Curr Opin Microbiol 5: 240–245

26. Ullman, WJ, Kirchman, DL, Welch, SA, Vandevivere, P (1996) Laboratory evidence for microbiologically mediated silicate mineral dissolution in nature. Chem Geol 132: 11–17

27. von Wintzingerode, F, Gobel, UB, Stackebrandt, E (1997) Determination of microbial diversity in environmental samples: pitfalls of PCR-based rRNA analysis. Microbiol Rev 21: 213–229

28. Welch, SA, Barker, WW, Banfield, JF (1999) Microbial extracellular polysaccharides and plagioclase dissolution. Geochim Cosmochim Acta 63: 1405–1419